Materials and Structures, 1993, **26**, 381–386

The fracture energy (G_F) of high-strength concretes

G. GIACCIO, C. ROCCO, R. ZERBINO

Dpto. Construcciones, Facultad de Ingeniería, UNLP. LEMIT-CIC. 1900 La Plata, Argentina

This paper presents results for the fracture energy of concrete (G_F) obtained from a wide range of high-strength concretes. Strength levels up to 100 MPa, aggregate type and aggregate surface texture were included as variables. The determination of G_F was performed according to the recommendation of the RILEM 50-FMC Committee. Compressive and tensile strengths and the modulus of elasticity are also presented. Measured values of G_F are compared with those proposed in the last CEB Model Code.

NOTATION

E	Modulus of elasticity
f'_c	Compressive strength
$f_{t(s)}$	Tensile strength (splitting test)
f_{net}	Modulus of rupture, central point loading (notched beams)
G_F	Fracture energy
MR	Modulus of rupture, four-point loading (unnotched beams)
δ_0	Maximum displacement
l_{ch}	Characteristic length

1. INTRODUCTION

Compressive strength is usually employed as the main parameter for the design of concrete structures. Nevertheless, as in other brittle materials, its fracture is governed by tensile mechanisms. Not only is strength important but so also is the whole behaviour of concrete under tensile stresses, especially its toughness. In many cases it would not be possible to build concrete structures that were safe enough if the material had no capacity to absorb energy.

Although fracture mechanics has been extensively developed for brittle materials, the applicability of conventional concepts to concrete is not easy, due to the characteristics of the material. Concrete is heterogeneous (a composite, multiphase material); cracking itself is a heterogeneous process (initiation of cracks, slow stable crack growth, crack arrest, and unstable crack propagation); the surface area formed is many times larger than the effective fracture area (multiple crack formation occurs) and as a consequence, the energy-dissipating mechanism in concrete is not merely confined to surface energy.

A specific method has been proposed by the RILEM Technical Committee TC-50 [1] to quantify the fracture energy G_F, and recommended values have been included in the last CEB Model Code [2].

At the same time the use of high-strength concretes is continuously increasing, but despite the amount of research that has been performed there are still many areas which need to be studied. Fracture toughness is one of them because questions about the 'brittleness' of high-strength concretes usually appear.

This paper presents results for the fracture energy of concrete G_F obtained from a wide range of high-strength concretes. The determination of G_F was performed according to the recommendation of the RILEM 50-FMC Committee. Results for the fracture energy of conventional concretes were presented before [3,4] as a contribution to the above-mentioned recommendation of RILEM, and major details of the testing methodology were included [1].

2. EXPERIMENTAL PROCEDURE

2.1 Materials

Concretes were prepared using different coarse aggregates and mix proportions. Three crushed stones with different petrographic characteristics – granite (G), basalt (B) and limestone (L) – and two river gravels (R-1 and R-2), with similar grading and different surface texture, were used as coarse aggregates. High-strength mixtures included high early-strength cement, siliceous river sand and superplasticizer.

Table 1 shows some characteristics of the mix proportions and the properties of fresh concretes. The effect of strength level can be analysed by comparing concretes which include granite as the coarse aggregate. Two concretes with river gravel are included to study the effect of the shape and surface texture of the aggregate. In the same way larger particles of gravel R-2 were crushed to obtain a similar particle size distribution (CR-2). Finally, a high-strength mortar and a normal-strength concrete are also included. Fig. 1 shows the particle size distributions of the different aggregates (fine aggregate + coarse aggregate).

Cylinders of 100 mm × 200 mm for compressive tests (compressive strength and modulus of elasticity) and beams of 100 mm × 100 mm × 840 mm for fracture energy and tensile tests were cast. Specimens were stored in water saturated with lime until testing.

Table 1 Mixtures

Mix	Coarse aggregate		Cement content (kg m^{-3})	SP[b]	Water/cement ratio	Consistency
	Volume (%)[a]	Type				
M	0	-	780	Yes	0.30	-
B	42	Basalt	495	Yes	0.28	Fluid
L	42	Limestone	450	Yes	0.30	Fluid
G-1, G-2	42	Granite	450	Yes[c]	0.30	Fluid
G-3	45	Granite	375	Yes	0.40	Fluid
N	40	Granite	250	No	0.75	Plastic
R-1	41	Gravel	460	Yes	0.30	Fluid
R-2	41	Gravel	460	Yes	0.30	Fluid
CR-2	41	Gravel[d]	460	Yes	0.30	Fluid

[a] Coarse aggregate volume/concrete volume.
[b] SP = superplasticizer admixture.
[c] Different dosage of admixture.
[d] Crushed river gravel.

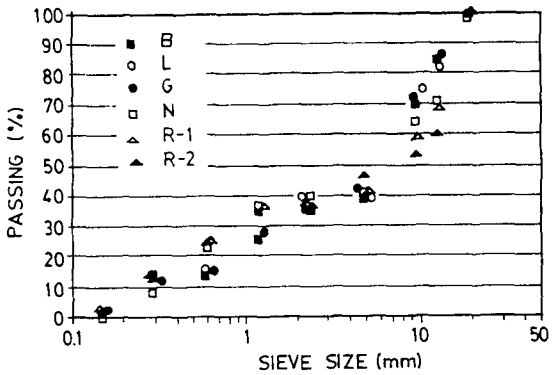

Fig. 1 Particle size distributions of the different aggregates.

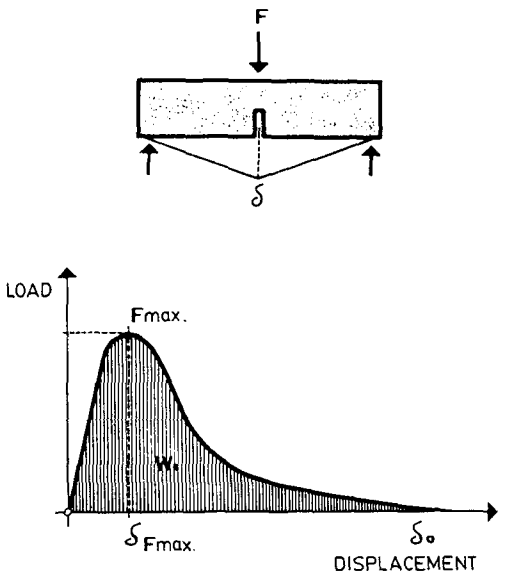

Fig. 2 Scheme of the test adopted to measure the energy of fracture G_F.

2.1 Testing methodology

The determination of G_F was performed according to the recommendation of the RILEM 50-FMC Committee. The load–displacement curve of sawn notched beams tested with central point loading over a span of 800 mm was measured. Tests were performed on a deformation-controlled testing machine. Fig. 2 schematizes the adopted test. Major details of testing procedure have been presented before [1].

The energy of fracture is calculated as

$$G_F = \frac{W_0 + mg\delta_0}{A_{lig}}$$

where W_0 is the area below the curve, $mg\delta_0$ the contribution of the weight of the beam, δ_0 the displacement at the final fracture of the beam, mg the weight (between the supports), and A_{lig} the cross-sectional area of the ligament (depth = 50 mm, width = 100 mm).

The net bending stress at maximum load (f_{net}) is calculated as

$$f_{net} = \frac{6[F_{max} + (mg/2)]l}{4bh^2}$$

where b is the width of the beam, h the net depth of the beam, l the span and F_{max} the maximum load.

The tensile strength was measured, after G_F tests, on the resulting broken halves of the beams: the flexural strength with four-point loading (over 300 mm span) and the splitting tensile strength were obtained. In some series the splitting tensile strength on 100 mm × 200 mm cylinders was also evaluated. Finally, the elastic modulus and the compressive strength were measured on cylinders.

3. RESULTS AND DICSUSSION

Table 2 shows test results for hardened concrete. Eight concretes with compressive strengths greater than 60 MPa are presented, together with a high-strength mortar and a low-strength concrete.

Concretes L, G-1, G-2, R-1, R-2 and CR-2 have a matrix similar to that of the mortar. Concretes L, G-1

Table 2 Results for hardened concrete

Mix	Cylinders			Notched beams			Unnotched beams[a]	
	f'_c (MPa)	E (GPa)	$f_{t(s)}$ (MPa)	f_{net} (MPa)	G_F (N m^{-1})	δ_0 (mm)	MR (MPa)	$f_{t(s)}$ (MPa)
M	79.3	39.1	–	7.2	75	0.6	11.8	7.0
B	106.6	58.2	6.2	9.7	205	1.2	11.2	6.2
L	63.5	38.2	–	7.4	180	1.4	8.9	4.9
G-1	86.6	41.4	–	7.4	195	1.5	8.7	5.1
G-2	78.7	40.8	–	7.0	185	1.5	8.7	4.3
G-3	70.8	40.0	–	6.3	175	1.5	7.2	4.1
N	22.7	28.8	–	4.1	135	1.7	4.4	2.3
R-1	68.2	56.2	4.7	7.5	150	1.4	8.1	4.7
R-2	72.2	48.3	4.9	8.4	170	1.2	8.8	5.2
CR-2	77.6	48.4	–	9.4	180	1.1	8.9	5.4

[a] Tests performed on halves of the notched beams after G_F test.

and G-2 achieve the same order of tensile strength; nevertheless the compressive strength is notably reduced in concrete L. In this case the strength limit is established by the aggregate. Many fractured aggregates appeared on the fracture surface (the above-mentioned differences in crack pattern and, consequently, in strength must be attributed to the particular characteristics of these calcareous aggregates, as there are many examples in the literature of high-strength concretes made with limestone). The three concretes achieved similar tensile strengths because they have similar matrices and matrix–aggregate bond strength. The effect of coarse aggregate was analysed before [5].

Concretes R-1 and R-2 have a lower compressive strength due to their round shape and smoother surface texture. Gravel R-1 is smoother than gravel R-2 (water absorption values after 24 h were 0.7 and 1.1% for R-1 and R-2, respectively). When gravel R-2 is crushed, an irregular but smoother shape is obtained. Concrete prepared with CR-2 increased the compressive strength by 7%. Differences in the shape and texture of aggregates produced changes in fracture surfaces, especially in R-1 which showed great amounts of interface (bond) cracks.

Concretes G-1 and G-2 have similar materials and mix proportions and their differences in strength are due to the greater air incorporation produced in G-2. Concrete B presents the highest strength.

The results of splitting tensile tests performed on cylinders and on beams showed very small differences.

Typical load–displacement curves are plotted in Fig. 3. Each curve corresponds to an individual test that best represents the mean behaviour of the series. Fig. 3a shows the behaviour of different strength-level concretes including the same coarse aggregate (granite). As the strength increases, concretes have a greater peak load deflection followed by a steeper gradient of the softening branch. However, differences in the load–displacement curves due to changes in strength are comparable to (or

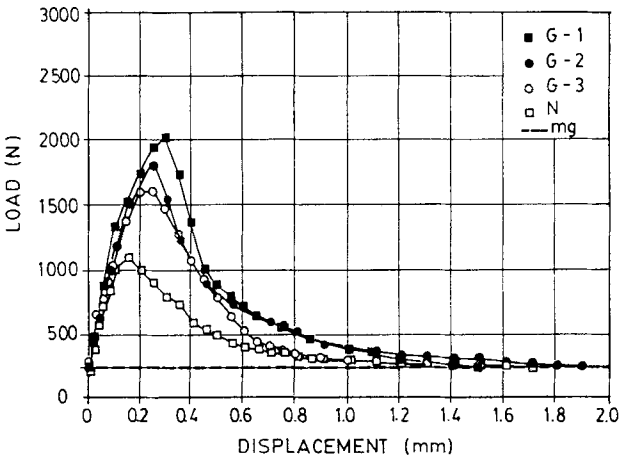

(a)

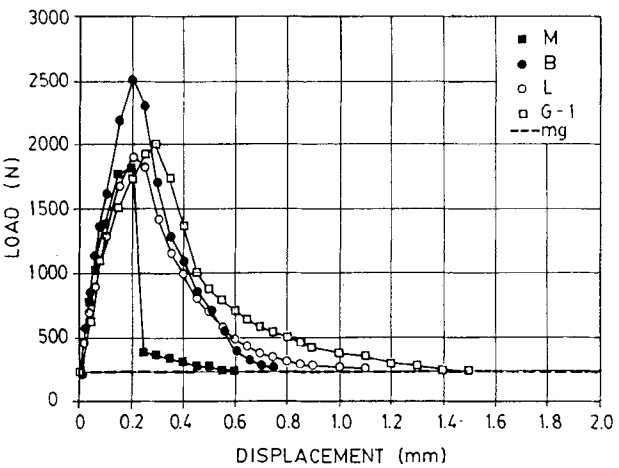

(b)

Fig. 3 Load–displacement curves for (a) concretes of different strength including granite, (b) mortar and concretes incorporating different coarse aggregates.

(continued)

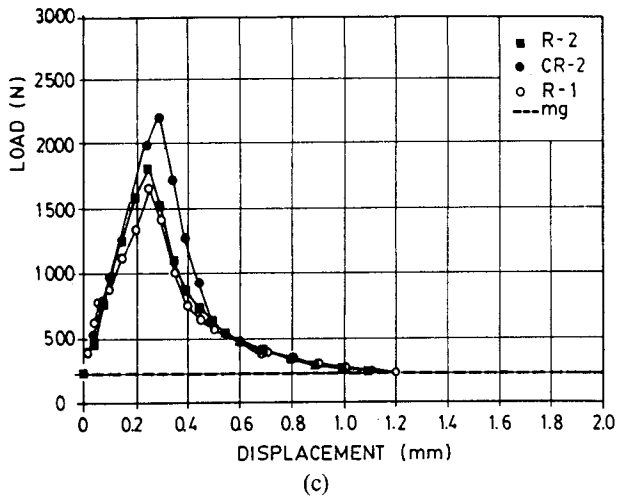

(c)

Fig. 3 Load–displacement curves (*continued*). (c) Gravel concretes.

smaller than) those which appear when the size of the coarse aggregate is modified [3]. Both variables (aggregate maximum size and strength level) affect the crack control capacity of concrete. Nevertheless, when a high-strength concrete and a normal concrete (which can include bigger aggregates) are compared, both phenomena are superposed.

Unlike the changes in the slope of the descending branch of the curve, the final displacements (δ_0) are similar for the different strengths.

Fig. 3b shows the load–displacement curves for mortar and concretes B, L and G-1. It can be seen that the final displacement is much lower for mortar than for concrete, and that it depends on the type of aggregate. Mortar presents the steepest gradient of the descending branch, followed by concrete B. The load–displacement curves of concretes are similar and the differences correspond to their differences in strength.

Fig. 3c shows the behaviour of gravel concretes. Concretes R-1 and R-2 show similar curves, the peak load and final displacement being smaller for R-1. Concrete CR-2 has the highest peak load (due to changes in aggregate shape) and the greatest slope of the softening branch.

The mean values of the energy of fracture G_F, calculated from the load–displacement curves, are reported in Table 2.

Fig. 4a and b shows the variation of the energy of fracture G_F with flexural and compressive strength, respectively. Fig. 4b also presents the values of G_F proposed by the last CEB Model Code [2].

The energy of fracture G_F increases as strength increases, even for high-strength concrete. However, as with tensile strength, the increment in G_F decreases as the strength level increases; thus the relative toughness (G_F/f'_c) decreases.

As expected, mortar has the smallest energy of fracture. The energy is strongly related to the aggregate size. For instance, it appears that a 16 mm high-strength concrete

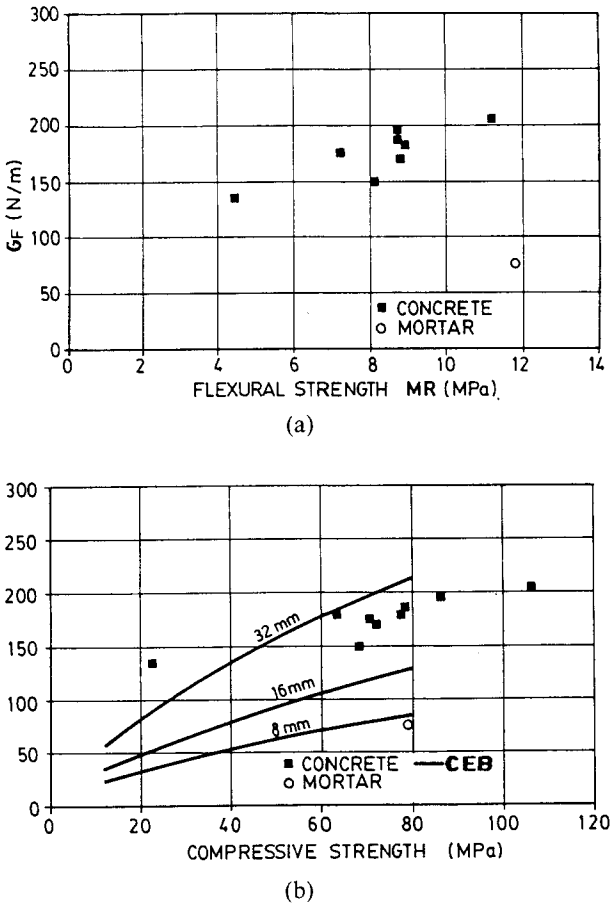

Fig. 4 Variation of the energy of fracture G_F with (a) flexural strength and (b) compressive strength.

can achieve similar values to a normal-strength concrete including coarser aggregates.

Fig. 4b shows that the experimental values (aggregate maximum size close to 16 mm) are included in the 'safe zone' and that they have a variation law similar to the proposed curve.

Differences in the energy of fracture produced by changes in the aggregate type are mainly related to variations in concrete strength. However, concrete R-1 prepared with the smoother gravel achieves the smallest value of G_F. The fracture energy mostly depends on the aggregate size.

Although the values of G_F achieve the same order for concretes prepared with different coarse aggregates and similar matrices, the observation of fracture surfaces makes evident that, especially in high-strength concretes, different failure mechanisms appear depending on the relative properties of aggregates, matrices and interfaces. In effect, tensile and compressive tests show that gravel concretes (e.g. R-1) only present debonding failure, while a sum of debonding and generally transgranular type of failure especially appears in L, G and B concretes.

From the proposed test of energy of fracture it is possible to estimate the tensile strength [6,7] and the characteristic length of the material ($l_{ch} = EG_F/f_t^2$), which is related to the sensitivity to cracking of the

Table 3 Tensile strength and characteristic lengths

Mix	Experimental values		Calculated values		
	f'_c (MPa)	$f_{t(s)}$ (MPa)	$f_{t(c)}$ (MPa)	$l_{ch}[f_{t(c)}]$ (mm)	$l_{ch}[f_{t(s)}]$ (mm)
M	79.3	7.0	6.7	65	60
B	106.6	6.2	6.1	330	310
L	63.5	4.9	4.6	325	285
G-1	86.6	5.1	4.4	415	310
G-2	78.7	4.3	4.1	480	410
G-3	70.8	4.1	3.5	570	415
N	22.7	2.3	2.1	880	735
R-1	68.2	4.7	4.4	435	380
R-2	72.2	5.2	5.4	280	300
CR-2	77.6	5.4	6.4	210	300

$f_{t(c)}$ = tensile strength obtained from G_F test.
$l_{ch}[f_{t(c)}]$ = characteristic length calculated using $f_{t(c)}$.
$l_{ch}[f_{t(s)}]$ = characteristic length calculated using $f_{t(s)}$.

material. (Tensile strength is obtained from the theoretical diagram presented by Hillerborg, which shows the variation of f_{net}/f_t = function of $h \times f^2_{net}/EG_F$.)

Table 3 shows estimated values of the tensile strength ($f_{t(c)}$) and the characteristic lengths calculated using $f_{t(c)}$ and the splitting tensile strength $f_{t(s)}$ measured on the halves of the beams.

There is a good correlation between experimental and calculated values of tensile strength. Experimental values tend to be slightly greater, while characteristic lengths calculated using $f_{t(s)}$ are generally smaller. However, as they have the same order, similar conclusions can be drawn by analysing the variation of any of them.

Fig. 5a and b shows the variations of characteristic length $l_{ch}[f_{t(s)}]$ with concrete flexural and compressive strength respectively. Similar conclusions can be drawn regarding $l_{ch}[f_{t(c)}]$.

It was verified that the characteristic lengths increase as the aggregate size increases, as can be seen by comparing the results for mortar and concretes. Characteristic lengths strongly decrease as concrete strength increases, and high-strength concretes present values two to three times smaller than the normal-strength concretes prepared with the same aggregates (G and N). As a consequence, linear elastic analysis is more applicable in high-strength concretes.

Fig. 5a shows that there is good correlation between l_{ch} and the flexural strength. On the other hand, when l_{ch} is plotted against compressive strength (Fig. 5b) a greater dispersion of values appears. The additional failure mechanisms (e.g. aggregate cracking) that can develop under the high stresses of a compressive load in high-strength concrete strongly limit the compressive strength. These mechanisms are not present (or at least are less significant) under tensile loading, and the characteristic lengths remain unaffected or only modified in a secondary manner. A worse correlation is then found under compressive loads as different mechanisms are being compared.

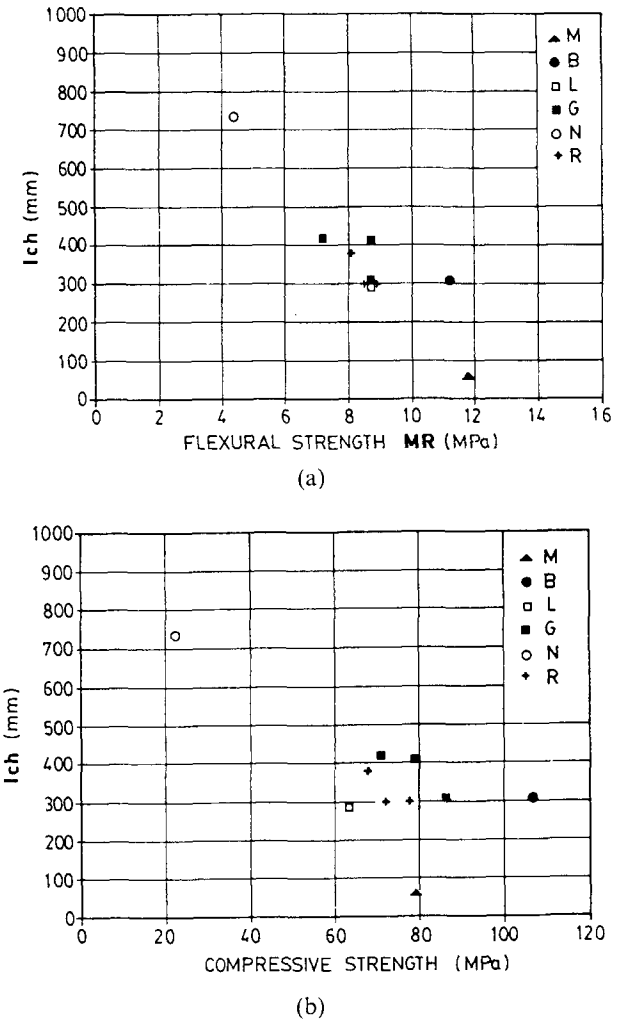

Fig. 5 Variation of the characteristic length $l_{ch}[f_{t(s)}]$ with (a) flexural strength and (b) compressive strength of concrete.

4. CONCLUSIONS

This paper presents results for the fracture energy of concrete obtained from a wide range of high-strength concretes. The following conclusions can be drawn.

It was verified that the energy of fracture depends on the aggregate size, the mortar having the smallest value.

The energy of fracture increases as concrete strength increases, even for high-strength concrete. However, as with tensile strength, the increments in the energy of fracture decrease as the strength level increases.

As the strength increases, concretes have a greater peak load deflection followed by a steeper gradient of the softening branch. The final displacements (δ_0) are similar for concretes with different strengths. The final displacement is much lower for mortar than for concrete, and it depends on the type (and size) of aggregate.

Characteristic lengths strongly decrease as concrete strength increases, and high-strength concretes present

values two to three times smaller than normal-strength concretes prepared with the same aggregate.

Finally, in high-strength concrete additional failure mechanisms can develop under compressive loading that are not present (or at least are less significant) under tensile loading.

REFERENCES

1. RILEM 50-FMC Committee (Fracture Mechanics of Concrete), 'Determination of the fracture energy of mortar and concrete by means of three-point bend tests on notched beams', *Mater. Struct.* **18**(106) (1985) 285–290.
2. CEB Model Code (1990).
3. Lima, L., Violini, D. and Zerbino, R., 'Energía de rotura del hormigón', in Proceedings, 6ª Reunión Técnica AATH, Bahía Blanca, November 1984, Vol. 2, pp. 385–410 (in Spanish).
4. Hillerborg, A., 'Results of three comparative test series for determining the fracture energy G_f of concrete', *Mater. Struct.* **18**(107) (1985) 407–413.
5. Giaccio, G., Rocco, C., Violini, D., Zappitelli, J. and Zerbino, R., 'High strength concretes incorporating different coarse aggregates', *Proc. ACI Mater. J.* **89**(3) (1992) 242–246.
6. Hillerborg, A., 'Concrete fracture energy tests performed by 9 laboratories according to a draft RILEM recommendation', Report TVBM-3015 (Division of Building Materials, Lund Institute of Technology, 1983).
7. *Idem.*, 'Additional concrete fracture energy tests performed by 6 laboratories according to a draft RILEM recommendation', Report TVBM-3017 (Division of Building Materials, Lund Institute of Technology, 1984).

RESUME

L'énergie de rupture G_F du béton de hautes performances

On analyse les résultats de l'énergie de rupture de bétons présentant des niveaux de résistance à la compression allant jusqu'à 100 MPa. On a déterminé l'énergie de rupture G_F selon la recommandation de la Commission Technique RILEM 50-FMC. Les principales variables étudiées étaient les suivantes: niveaux de résistance, types et textures des granulats. On analyse les propriétés des mélanges obtenus avec différents types de gros granulats et une distribution granulométrique égale: trois granulats concassés (basalte, granit et calcaire) et deux graviers. On a mesuré aussi la résistance à la compression, le module d'élasticité et la résistance à la traction par fendage et par flexion de chaque béton. On a vérifié l'influence de la dimension des granulats sur l'énergie de rupture G_F, laquelle augmente encore avec la résistance du béton dans les domaines de haute résistance. Pour les bétons avec des granulats de 16 mm, on a mesuré des valeurs de l'énergie de rupture G_F proches de 200 N m^{-1}. Les résultats obtenus sont comparés avec les valeurs indiquées dans le dernier Model Code du CEB.